Published in final edited form as:
J Biol Inorg Chem. 2013 October ; 18(7): 779–790. doi:10.1007/s00775-013-1024-2.

The Metal-Drug Synergy: New Ruthenium^{II} Complexes of Ketoconazole are Highly Active against *Leishmania major* and *Trypanosoma cruzi* and Non-toxic to Human or Murine Normal Cells

Eva Iniguez[†], **Antonio Sánchez**[§], **Miguel A. Vasquez**[†], **Alberto Martínez**[‡], **Joanna Olivas**[†], **Aaron Sattler**[¶], **Roberto A. Sánchez-Delgado**[§,✉], and **Rosa A. Maldonado**[†,✉]

[†]Border Biomedical Research Center, Department of Biological Sciences, The University of Texas at El Paso, El Paso, TX 79968, USA

[§]Chemistry Department, Brooklyn College and The Graduate Center, The City University of New York, 2900 Bedford Avenue, Brooklyn, NY 11210, USA

[‡]Chemistry Department, New York City College of Technology, The City University of New York, Brooklyn, NY 11201, USA

[¶]Department of Chemistry, Columbia University, 3000 Broadway, New York, NY 10027, USA

Abstract

In our ongoing search for new metal-based chemotherapeutic agents against leishmaniasis and Chagas disease, six new ruthenium-ketoconazole (Ru-KTZ) complexes have been synthesized and characterized, including two octahedral coordination complexes *cis-fac*-[$Ru^{II}Cl_2(DMSO)_3(KTZ)$] (**1**) and *cis*-[$Ru^{II}Cl_2$(bipy)(DMSO)(KTZ)] (**2**), and four organometallic compounds [Ru^{II}(η^6-*p*-cymene)Cl_2(KTZ)] (**3**), [Ru^{II}(η^6-*p*-cymene)(en)(KTZ)][BF_4]$_2$ (**4**), [Ru^{II}(η^6-*p*-cymene)(bipy)(KTZ)][BF_4]$_2$ (**5**), and [Ru^{II}(η^6-*p*-cymene)(acac)(KTZ)][BF_4] (**6**); the crystal structure of (**3**) is described. The central hypothesis of our work is that combining a bioactive compound like KTZ and a metal in a single molecule results in a synergy that can translate into improved activity and/or selectivity against parasites. In agreement with this hypothesis, complexation of KTZ to Ru^{II} in compounds **3**-**5** produces a marked enhancement of the activity toward promastigotes and intracellular amastigotes of *Leishmania major*, when compared with uncomplexed KTZ, or with similar Ru compounds not containing KTZ. Importantly, the selective toxicity of compounds **3**-**5** toward the leishmania parasites, in relation to human fibroblasts and osteoblasts, or murine macrophages, is also superior to those of the individual constituents of the drug. When tested against *Trypanosoma cruzi* epimastigotes, some of the organometallic complexes displayed an activity and selectivity comparable to that of free KTZ. A dual-target mechanism is suggested to account for the antiparasitic properties of these complexes.

Keywords

Leishmaniasis; Chagas; Ketoconazole; Ruthenium; Metal-Drug Synergy

✉R. A. Sánchez-Delgado, RSdelgado@brooklyn.cuny.edu; Rosa A. Maldonado, ramaldonado@utep.edu.

Introduction

Leishmaniasis is one of the world's most neglected diseases, affecting mainly the poorest populations of developing countries. This disease, caused by more than 20 species and subspecies of a hemoflagellate protozoan of the genus *Leishmania*, is endemic in 88 countries; some 2 million new cases occur yearly and 350 million people are considered at risk of contracting leishmaniasis [1, 2]. American Trypanosomiasis (Chagas' disease), caused by *Trypanosoma cruzi* [3], is also largely neglected by public health programs, media and pharmaceutical companies; it affects over 20 million people in Central and South America, of which up to 5 million develop severe digestive and cardiac impairments, causing 10-15,000 deaths per year and a heavy burden of persons unable to work [4-7].

Leishmaniasis has been traditionally treated with pentavalent antimonial compounds like pentostam and glucantime, or with amphotericin B in unresponsive cases, while the chemotherapy of Chagas disease typically employs benznidazole or nifurtimox. These treatments suffer, in most of cases, from toxicity problems, limited efficacy, and emerging resistance; thus, the search for novel chemotherapeutic agents for these ailments clearly requires urgent attention. Over the last several years we have demonstrated the efficacy of the metal-drug synergy [8, 9] in searching for new therapies against *Trypanosoma cruzi* and *Leishmania major*; the approach involves combining a compound of known anti-parasitic activity and a metal in a single molecule. The resulting metal-based drugs display enhanced activity and reduced toxicity to mammalian cells, when compared to their individual constituents. These favorable features are the result of improved physicochemical properties and of novel mechanisms of action involving dual or multiple targets [8, 9]. Our strategy makes use of the fact that sterol 14-demethylases have been validated as chemotherapeutic targets for trypanosomatids; in particular, azole and triazole compounds cause a depletion of normal sterols and an accumulation of abnormal amounts of sterol precursors with cytostatic or cytotoxic consequences [10-16]. We have demonstrated that attaching such azole-type sterol biosynthesis inhibitors (SBIs), specifically clotrimazole (CTZ) or ketoconazole (KTZ) to metal-containing fragments (Ru, Rh, Ir, Au and Cu) effectively enhances their activity against *T. cruzi*, while maintaining a low toxicity for mammalian cells [17-20].

Other researchers have described a number of metal derivatives with interesting anti-Chagas and anti-leishmanial activity targeting different biochemical pathways; they include complexes of Pd, Pt and Ru with nitrofuran thiosemicarbazones, pentamidine, pyridine-2-thiol-N-oxyde, dithiocarbazates, or aryl-4-oxothiazolylhydrazones [21-25]. Rh-, Ir-, Pt- and Cu-containing moieties coordinated to pentamidine, or to the DNA intercalator dipyrido[3,2-a:2′,3′-c]phenazine (dppz) [8, 9, 26-28], and cyclometallated Au, Pd, and Re derivatives with cathepsin B inhibitory ability [29] have also shown interesting activity.

Recently we reported a remarkable series of organometallic compounds containing Ru^{II} and CTZ, which display unprecedentedly high in vitro antiparasitic activity combined with very low toxicity toward normal mammalian cells [30]. In particular, the complex [Ru^{II}(η⁶-*p*-cymene)Cl_2(CTZ)] shows an enhancement of the activity of CTZ by a factor of 110 against *L. major* promastigotes and by 58 against *T. cruzi* epimastigotes, resulting in low nanomolar and low micromolar lethal doses, respectively. In addition, [Ru^{II}(η⁶-*p*-cymene)Cl_2(CTZ)] does not exhibit any appreciable toxicity to human osteoblasts when assayed up to 7.5 μM, which translates into excellent selectivity indexes higher than 500 for *L. major* and 75 for *T. cruzi*. This compound also significantly inhibited the proliferation of intracellular amastigotes of *L. major* in infected intraperitoneal mice macrophages (IC_{70} 29 nM). In vivo testing and detailed mechanistic studies of these Ru-CTZ complexes are currently in progress.

In this paper we describe further work aimed at discovering new leads for possible chemotherapies against leishmaniasis and Chagas. Six new ruthenium-based compounds containing KTZ have been synthesized and characterized, including two coordination complexes, *cis-fac*-[$Ru^{II}Cl_2(DMSO)_3$(KTZ)] (**1**) and *cis*-[$Ru^{II}Cl_2$(bipy)(DMSO)(KTZ)] (**2**), and four organometallic complexes [Ru^{II}(η^6-*p*-cymene)Cl_2(KTZ)] (**3**), [Ru^{II}(η^6-*p*-cymene)(en)(KTZ)][BF_4]$_2$ (**4**), [Ru^{II}(η^6-*p*-cymene)(bipy)(KTZ)][BF_4]$_2$ (**5**) and [Ru^{II}(η^6-*p*-cymene)(acac)(KTZ)][BF_4] (**6**) (bipy = bipyridine; en = ethlylenediamine; acac = acetylacetonate). In vitro assays reveal a marked enhancement of the activity against *L. major* promastigotes and amastigotes for complexes **3**-**5**, when compared with KTZ or with similar Ru compounds not containing KTZ, together with a low toxicity toward mammalian cells. When tested against *Trypanosoma cruzi* epimastigotes, some of the organometallic complexes displayed an activity and selectivity comparable to that of KTZ.

Materials and Methods

Materials

$RuCl_3 \cdot 3H_2O$ (Pressure Chemicals) and all organic compounds were used as received. Solvents were purified using a PureSolv purification unit from Innovative Technology, Inc. All manipulations were carried out under dry nitrogen using standard Schlenk techniques. [Ru^{II}(η^6-*p*-cymene)Cl_2]$_2$ [31], [Ru^{II} (η^6-*p*-cymene)(en)Cl][BF_4] [32], [Ru^{II}(η^6-*p*-cymene)Cl(acac)] [33], and *cis*-[$Ru^{II}Cl_2(DMSO)_4$] [34] were prepared according to published procedures. Elemental analyses were performed by Atlantic Microlabs Inc., Norcross, Georgia. NMR spectra were obtained on a Bruker AVANCE 400 spectrometer. Chemical shifts were recorded relative to residual proton or carbon resonances in the deuterated solvents. The atom numbering used in the NMR spectra are shown in Fig. 1 (*bi* and *cy* prefixes are used in NMR nomenclature when referring to bipyridine and *p*-cymene, respectively).

Syntheses of Ruthenium-Ketoconazole compounds

cis,fac-[$Ru^{II}Cl_2(DMSO)_3$(KTZ)] (1)—*cis*-[$Ru^{II}Cl_2(DMSO)_4$] (0.20 g, 0.41 mmol) and KTZ (0.22 g, 0.41 mmol) were stirred in dichloromethane (10 mL) under N_2 for 20 h at room temperature. The yellow solution was concentrated under vacuum to approximately 2 mL and diethyl ether (20 mL) was added to yield a pale yellow solid. After filtration, the product was washed with diethyl ether (3×20 mL) and dried under vacuum. Yield 0.302 g, 79%. ^{1}H NMR ($CDCl_3$, 400 MHz) δ(ppm): 8.53 (bt,1H, H_2), 7.75 (bt, 1H, H_5), 7.55 (d, J= 8 Hz, 1 H, H_8), 7.45 (d, J= 4 Hz, 1H, H_{11}), 7.22 (dd, J= 8 Hz, J'= 4 Hz, 1H, H_9), 6.92 (bt, 1H, H_4), 6.88 (s, 4H, H_{21}, H_{22}, H_{25}, H_{23}), 4.55 (d, J= 15 Hz, 1H, H_6), 4.47 (d, J= 15 Hz, 1H, H_6), 4.32 (m, 1H, H_{15}), 4.00 (m, 1H, H_{18}), 3.93 (pt, 1H, H_{16}), 3.75 (m, 1H, H_{16}), 3.75 (m, 2H, H_{28}, H_{30}), 3.70 (m, 1H, H_{18}), 3.61 (m, 2H, H_{28}, H_{30}), 3.49 (s, 6H, Me-$DMSO_{trans}$), 3.40 (s, 6H, Me-$DMSO_{cis}$), 3.15 (s, 3H Me-$DMSO_{cis}$), 3.14 (s, 3H Me-$DMSO_{cis}$), 3.06-2.98 (m, 4H, H_{27}, H_{31}), 2.13 (s, 3H, H_{33}); ^{13}C NMR ($CDCl_3$, 100MHz) δ(ppm): C(32) 168.95, C(10,12) 152.98, 145.79, C(2) 143.97, C(7,20,25) 136.03, 134.08, 133.05, C(11) 131.43, C(5) 130.50, C(8) 129.66, C(9) 127.20 C(4) 120.38, C(21,22,23,24) 118.80, 115.75, C(13) 107.73, C(15) 75.10, C(18) 68.32, C(16) 67.73, C(6) 52.56, C(27,31) 51.10, 50.70, C($DMSO_{cis}$) 48.08, 48.04, 46.83, C(28,30) 46.37, 41.48, C($DMSO_{trans}$) 46.18, C(33) 21.28. Anal. Calcd for $C_{32}H_{46}Cl_4N_4O_7RuS_3 \cdot H_2O$ C, 40.21; H, 5.06; N, 5.86. Found: C, 40.21; H, 4.83; N, 5.75.

cis-[$Ru^{II}Cl_2$(bipy)(DMSO)(KTZ)] (2)—*cis*-[$Ru^{II}Cl_2(DMSO)_4$] (0.10 g, 0.20 mmol) was stirred in THF (20 mL) at room temperature for 5 minutes, then bipy (0.032 g 0.20 mmol) was added and the resulting yellow suspension was refluxed overnight (12 h); orange solid *cis-cis*-[$Ru^{II}Cl_2(DMSO)_2$(bipy)] precipitated [35]. The solution was allowed to cool to room

temperature; the solid was filtered off, washed with THF and diethyl ether, and dried under vacuum. *cis-cis*-[$Ru^{II}Cl_2(DMSO)_2$(bipy)] was dissolved in chloroform (20 mL) and an equimolar amount of KTZ (0.107 g, 0.20 mmol) was added. The resulting orange solution was refluxed for 17 h, producing a brown solution that was cooled down and concentrated to a volume of approximately 2 mL. Addition of hexane (20 mL) led to the formation of a light brown oil. The solvent was decanted off and more hexane (20 mL) was added and decanted. This operation was repeated until the oil turned into a light brown solid, which was filtered off, washed with diethyl ether and dried in vacuum. Yield 0.122 g, 65%. ^{1}H NMR ($CDCl_3$, 400 MHz) δ(ppm): 9.90 (bd, 2H, $H_{bi5,5'}$), 8.09 (bt,1H, H_2), 7.91 (pt, *J* = 8 Hz, 2H, $H_{bi2,2'}$) 7.80-7.72 (m, 2H, $H_{bi3,3'}$), 7.47 (d, *J* = 8 Hz, 1H, H_8), 7.38-7.29 (m, 3H, H_{11} + $H_{bi4,4'}$), 7.18 (dd, *J* = 8 Hz, *J'* = 4 Hz, 1H, H_9), 6.90 (m, 4H, H_{21}, H_{22}, H_{25}, H_{23}), 6.68 (bt, 1H, H_5), 6.24 (bt, 1H, H_4), 4.37 (d, *J* = 12 Hz, 1H, H_6), 4.28 (d, *J* = 12 Hz, 1H, H_6), 4.23 (m, 1H, H_{15}), 3.90 (m, 1H, H_{18}), 3.80 (bt, 2H, H_{28}, H_{30}), 3.80 (m, 1H, H_{16}), 3.66 (bs, 2H, H_{28}, H_{30}), 3.54 (m, 1H, H_{16}), 3.29 (m, 1H, H_{18}), 3.18 (s, 3H Me-DMSO), 3.17 (s, 3H Me-DMSO), 3.10 (bt, 4H, H_{27}, H_{31}), 2.17 (s, 3H, H_{33}); ^{13}C NMR ($CDCl_3$, 100MHz) δ(ppm): C(32) 168.97, C(Bi1) 160.29, C(Bi5) 155.03, C(10,12,7) 135.76, 134.23, 132.90 C(2) 142.39, C(Bi3) 134.50, C(11) 131.23, C(8) 129.55, C(9) 127.13, C(5) 126.84, C(Bi4) 125.32, C(Bi2) 121.55, C(4) 121.08, C(21,22,23,24) 118.82, 115.75, C(13) 107.65, C(15) 74.71, C(18) 68.10, C(16) 67.94, C(6) 52.19, C(27,31) 50.81, 50.79, C(28,30) 46.39, 41.63, C(Me-DMSO) 43.73, C(33) 21.32. Anal. Calcd for $C_{38}H_{42}Cl_4N_6O_5RuS{\cdot}H_2O$ C, 47.76; H, 4.64; N, 8.79. Found: C, 47.47; H, 4.66; N, 8.41.

[Ru^{II}(η^6-p-cymene)Cl_2(KTZ)] (3)—To a suspension of [Ru^{II}(η^6-*p*-cymene)Cl_2]$_2$ (0.10 g, 0.16 mmol) in acetone (20 mL), KTZ (0.17 g 0.32 mmol) was added. The mixture was stirred for 3.5 h at room temperature until the solution turned into a clear brownish-orange color; then the volume was reduced to approximately 2 mL under vacuum. Addition of diethyl ether (20 mL) yielded a light brown precipitate that was filtered, washed with diethyl ether and dried under vacuum. Yield 0.213 g, 80%. ^{1}H NMR ($CDCl_3$, 400 MHz) δ(ppm): 7.95 (bt,1H, H_2), 7.58 (d, *J* = 8 Hz, 1H, H_8), 7.48 (d, *J* = 4 Hz, 1H, H_{11}), 7.28 (dd, *J* = 8 Hz, *J'* = 4 Hz, 1H, H_9), 7.26 (bt, 1H, H_5), 6.94 (bt, 1H, H_4), 6.90 (m, 4H, H_{21}, H_{22}, H_{25}, H_{23}), 5.40 (pt, *J* = 8 Hz, 2H, $H_{cy3,4}$), 5.20 (d, *J* = 8 Hz, 2H, $H_{cy1,2}$), 4.49 (d, *J* = 16 Hz, 1H, H_6), 4.38 (d, *J* = 16 Hz, 1H, H_6), 4.34 (m, 1H, H_{15}), 3.90 (m, 1H, H_{16}), 3.88 (m, 1H, H_{18}), 3.77 (bt, 2H, H_{28}, H_{30}),3.72 (m, 1H, H_{16}), 3.61 (m, 2H, H_{28}, H_{30}), 3.57 (m, 1H, H_{18}), 3.08-2.93 (m, 4H, H_{27}, H_{31}), 2.95 (hpt, *J* = 12 Hz, 1H, H_{ip}), 2.15 (s, 6H, H_{33} + Me_{cy}), 1.25 (d, *J* = 12 Hz, 6H, Me_{ip}); ^{13}C NMR ($CDCl_3$, 100MHz) δ(ppm): C(32) 168.96, C(10,12) 152.93, 145.75, C(2) 142.12, C(7,20,25) 136.08, 134.17, 133.05 C(11) 131.40, C(5) 131.07, C(8) 129.64, C(9) 127.27 C(4) 121.54, C(21,22,23,24) 118.80, 115.77, C(7,Cy1, Cy4) 107.62, 102.42, 97.31 C(Cy2, Cy3) 82.79, 81.25, C(15) 75.16, C(18) 68.31, C(16) 67.67, C(6) 52.32, C(27,31) 51.04, 50.71, C(28,30) 46.41, 41.52, C(^{i}Pr) 30.68, C(33, Me1-^{i}Pr, Me2-^{i}Pr, Me-cy) 22.28, 22.22, 22.14, 21.30. Anal. Calcd for $C_{36}H_{42}Cl_4N_4O_5Ru{\cdot}H_2O$ C, 50.53; H, 5.18; N, 6.55. Found: C, 50.76; H, 5.01; N, 6.40.

[Ru^{II}(η^6-p-cymene)(en)(KTZ)][BF_4]$_2$ (4)—[Ru^{II}(η^6-*p*-cymene)Cl(en)][BF_4] (0.76 g, 1.81 mmol) was dissolved in acetone (20 mL) and $AgBF_4$ (0.39 g, 1.98 mmol) was added. Precipitation of AgCl was observed while the solution turned brown. After removal of AgCl by filtration, KTZ (0.97 g, 1.83 mmol) was added and the mixture stirred at room temperature for 2 h. The resulting brown suspension was filtered, and the filtrate evaporated to dryness. The product was extracted with CH_2Cl_2 (25 mL), concentrated to approximately 2 mL and precipitated by addition of hexane (20 mL). The yellow product was washed several times with hexane and diethyl ether and dried under vacuum. Yield 1.194 g, 66%. ^{1}H NMR (CD_3COCD_3, 400 MHz) δ(ppm): 8.34 (bt,1H, H_2), 7.76 (d, *J* = 8 Hz, 1H, H_8), 7.61 (d, *J* = 4 Hz, 1H, H_{11}), 7.45 (dd, *J* = 8 Hz, *J'* = 4 Hz, 1H, H_9), 7.44 (bt, 1H, H_4), 7.38 (bt,

1H, H_5), 7.00 (d, J = 8 Hz, 2H, H_{22}, H_{23}), 6.96 (d, J = 8 Hz, 2H, H_{21}, H_{25}), 6.08(bs, 2H, $enNH_2$), 5.88 (pt, J = 8 Hz, 2H, $H_{cy1,2}$), 5.81 (d, J = 8 Hz, 2H, $H_{cy3,4}$), 4.80(s, 2H, H_6), 4.50 (m, 1H, H_{15}), 4.11 (bs, 2H, $enNH_2$), 4.08-3.96 (m, 4H, H_{16}+H_{18}), 3.65 (bt, 4H, H_{28}, H_{30}), 3.15-2.93 (m, 4H, H_{27}, H_{31}), 2.66 (3H, H_{ip}+$enCH_2$), 2.19 (s, 3H, Me_{cy}), 2.13 (s, 3H,, H_{33}), 1.23 (pt, J = 8 Hz, 6H, Me_{ip}); ^{13}C NMR (CD_3COCD_3, 100MHz) □(ppm): C(32) 168.03, C(10,12) 152.75, 146.48, C(2) 143.01, C(7,20,25) 135.48, 134.56, 133.08, C(11) 131.06, C(8) 129.64, C(4) 129.76, C(9) 127.77, C(5) 124.22, C(21,24) 118.42, C(22,23) 115.64, C(13,Cy1, Cy4) 107.54, 106.46, 100.03, C(Cy2, Cy3) 83.60, 83.57, C(15) 75.19, C(18) 68.41, C(16) 66.90, C(6) 52.17, C(27,31) 50.76, 50.32, C(28,30) 46.02, 41.09, C(en) 45.01, C(^{i}Pr) 30.23, C(Me1-^{i}Pr, Me2-^{i}Pr,) 21.87, 21.80, C(33) 20.41, C(Me-Cy) 17.15. Anal. Calcd for $C_{38}H_{50}Cl_2N_6O_4RuB_2F_8$ C, 45.62; H, 5.04; N, 8.40. Found: C, 45.52; H, 5.44; N, 7.91.

[Ru^{II}(η^6-p-cymene)(bipy)(KTZ)][BF_4]$_2$ (5)—To a suspension of [Ru^{II}(□^{6}-*p*-cymene)Cl_2]$_2$ (0.10 g, 0.16 mmol) in acetone (20 mL), $AgBF_4$ (0.13 g 0.64 mmol) was added. The color changed from dark brownish red to light orange and the appearance of AgCl was observed. The suspension was stirred at RT for 3 h and then filtered; the resulting orange solution was cooled to −20 °C for 72 h to complete the precipitation of AgCl. After filtration, bipyridine (0.05 g, 0.32 mmol) was added and the mixture stirred at room temperature for 3 h. The brown solution was concentrated to approximately 2 mL and hexane (20 mL) was added to produce a dark-brown oil. The hexane layer was decanted and the addition and decantation of successive hexane portions (20 mL) yielded a brownish-orange solid that was dried under vacuum and re-dissolved in CH_2Cl_2. KTZ (0.17 g, 0.32 mmol) was added and the solution was stirred at room temperature for 1h, then concentrated to a volume of approximately 2 mL. Addition of hexane (20 mL) yielded the product as a light brown precipitate that was washed with hexane and diethyl ether, and finally dried under vacuum. Yield 0.302 g, 87%. ^{1}H NMR (CD_2Cl_2, 400 MHz) □(ppm): 9.89 (pt, J = 12 Hz, 2H, $H_{bi5,5}$), 8.46-7.41m (m, 6H, $H_{bi2,2}$ + $H_{bi3,3}$ + $H_{bi4,4}$) 7.81 (bt,1H, H_2), 7.39 (d, J = 4 Hz, 1H, H_{11}), 7.37 (d, J = 8 Hz, 1H, H_8), 7.18 (dd, J = 8 Hz, J' = 4 Hz, 1H, H_9), 6.96 (d, J = 9 Hz, 2H, H_{22}, H_{23}), 6.89(bt, 1H, H_5), 6.76(d, J = 9 Hz, 2H, H_{21}, H_{25}), 6.64 (bt, 1H, H_4), 6.31 (pt, J = 5 Hz, 2H, $H_{cy1,2}$), 6.15 (d, J = 5 Hz, 2H, $H_{cy3,4}$), 4.56-4.46 (m, 2H, H_6), 4.21 (m, 1H, H_{15}), 3.81 (m, 1H, H_{16}), 3.75 (bt, 2H, H_{28}, H_{30}), 3.71 (m, 1H, H_{18}), 3.66 (m, 2H, H_{28}, H_{30}), 3.52 (m, 1H, H_{16}), 3.45 (m, 1H, H_{18}), 3.13-3.06 (m, 4H, H_{27}, H_{31}), 2.43 (hpt, J = 6 Hz, 1H, H_{ip}), 2.12 (s, 3H, H_{33}), 1.89 (s, 1H, Me_{cy}), 0.93 (d, J = 6 Hz, 6H, Me_{ip}); ^{13}C NMR (CD_2Cl_2, 100MHz) □(ppm): C(32) 168.66, C(Bi5) 157.00, C(Bi1,10,12) 154.41, 152.48, 146.29, C(2) 142.04, C(Bi2,Bi3,Bi4) 140.53, 129.44, 123.40, C(7,20,25) 135.78, 133.44, 132.99, C(11) 131.20, C(5) 129.81, C(8) 129.41, C (4) 128.60, C(9) 127.06, C(21,22) 118.46, C(23,24) 115.50, C(13, Cy1, Cy4) 109.30, 107.21, 104.63, C(Cy2) 91.50, C(Cy3) 83.90, C(15) 74.73, C(18) 67.83, C(16) 66.98, C(6) 52.33, C(27,31) 50.68, 50.39, C(28,30) 46.30, 41.33, C(^{i}Pr) 31.10, C(Me1-^{i}Pr, Me2-^{i}Pr) 21.98, 21.95, C(33) 21.08, C(Me-cy) 17.98. Anal. Calcd for $C_{46}H_{50}Cl_2N_6O_4RuB_2F_8$ C, 50.39; H, 4.60; N, 7.66. Found: C, 50.77; H, 4.82; N, 7.49.

[Ru^{II}(η^6-p-cymene)(acac)(KTZ)][BF_4] (6)—[Ru^{II}(□^{6}-*p*-cymene)Cl(acac)] (0.18 mg, 0.24 mmol) was dissolved in acetone (20 mL) and $AgBF_4$ (0.13 g 0.26 mmol) was added. The resulting suspension was stirred at room temperature for 2 h. The solvent was removed under vacuum and the residue was extracted with dichloromethane and filtered. To the resulting yellow solution, KTZ (0.14 g 0.26 mmol) was added and the mixture stirred at room temperature for 12 h. The resulting greenish yellow solution was filtered and concentrated under vacuum to a volume of approximately 2 mL. The product was precipitated by addition of hexane (20 mL) to yield a fine yellow powder that was washed with hexane and diethyl ether, and dried under vacuum. Yield 0.148 g, 60%. ^{1}H NMR ($CDCl_3$, 400 Hz) □(ppm): 7.79 (bt,1H, H_2), 7.51(d, J = 8 Hz, 1H, H_8), 7.41 (d, J = 3 Hz, 1H,

H_{11}), 7.19 (dd, J = 8 Hz, J' = 3 Hz, 1H, H_9), 6.90 (d, J = 9.5 Hz, 2H, H_{22}, H_{23}), 6.89 (bt, 1H, H_4), 6.83 (d, J = 9.5 Hz, 2H, H_{21}, H_{25}), 6.59 (bt, 1H, H_5), 5.57 (d, J = 6 Hz, 2H, $H_{cy1,2}$), 5.44 (d, J = 6 Hz, 2H, $H_{cy3,4}$), 4.92 (s, 1H, H_{acac}), 4.70 (d, J = 15 Hz, 1H, H_6), 4.60 (d, J = 15 Hz, 1H, Im H_6), 4.30 (m, 1H, H_{15}), 3.93, 3.63 (m, 2H, H_{16}), 3.88, 3.50(m, 2H, H_{18}), 3.77 (bt, 2H, $H_{28,}$ H_{30}), 3.63 (bt, 2H, $H_{28,}$ H_{30}), 3.08 (bt, 2H, $H_{27,}$ H_{31}), 3.03 (bt, 2H, $H_{27,}$ H_{31}), 2.74 (hpt, J = 7 Hz,1H, H_{ip}), 2.15 (s, 3H, H_{33}) 2.06 (s, 3H, Me_{cy}), 1.91, 1.85 (s, 6H, 2xMe_{acac}), 1.27 (pt, J = 7 Hz, 6H, Me_{ip}); ^{13}C NMR ($CDCl_3$, 100MHz) δ(ppm): C(CO-acac) 187.31, C(32) 168.98, C(10,12) 152.87, 145.90, C(2) 141.04, C(7,20,25) 135.85, 133.98, 132.93, C(11) 131.16, C(8) 129.94, C(4) 127.22, C(9) 127.12, C(5) 122.02, C(21,24) 118.76, C(22,23) 115.59, C(7,Cy1, Cy4) 107.68, 101.70, 98.67, C(CH-acac) 98.98, C(Cy2) 83.77, 83.70, C(Cy3) 81.05,81.00, C(15) 74.66, C(18) 68.18, C(16) 67.59, C(6) 52.34, C(27,31) 50.97, 50.68, C(28,30) 46.38, 4148, C(^{i}Pr) 30.68,C(Me-acac) 27.04, 27.02 C(Me1-^{i}Pr, Me2-^{i}Pr) 22.14, C(33) 21.29, C(Me-Cy) 17.29. Anal. Calcd for $C_{41}H_{49}Cl_2N_4O_6RuBF_4$ C, 51.69; H, 5.18; N, 5.88. Found: C, 51.12; H, 5.27; N, 6.01.

X-ray structure determination of complex 3

X-ray diffraction data were collected on a Bruker Apex II diffractometer. Crystal data, data collection and refinement parameters are summarized in Table 1. A CIF file has been deposited with Cambridge Crsytallographic Data Centre (CCDC). CCDC 926335 contains the supplementary crystallographic data for this paper. These data can be obtained free of charge from The Cambridge Crystallographic Data Centre via www.ccdc.cam.ac.uk/data_request/cif. The structure was solved using direct methods and standard difference map techniques, and refined by full-matrix least-squares procedures on $F2$ with SHELXTL (Version 6.10) [36, 37].

Biological Activity

Trypanosomatid cultures

Epimastigote forms of *T. cruzi* Y strain (*TcLuc-RAM*) were grown in liver infusion-tryptose (LIT, #45) medium [38]. Promastigote forms of *L. major* strain Friedlin clone V1 (*Lm*-luc) were grown in RPMI 1640 medium supplemented with hemin and 10% fetal bovine serum inactivated at 56°C for 30 min [39].

Culture of mammalian cells

Human osteoblast U205 (ATCC # CRL-2496), Hs27 human fibroblast (ATCC # HTB-99), and mouse macrophage Raw 264.7 (ATCC # TIB-71) (American Type Culture Collection, Manassas, Virginia) cells were cultured in Dulbecco's Modified Eagle's Medium (DMEM), supplemented with 10% inactivated FBS**,** along with 1% of 10,000 units/ml penicillin and 10 mg/ml streptomycin**,** in 0.9% sodium chloride. Cell cultures were regularly tested for *Mycoplasma* by polymerase chain reaction (PCR) [40]. Intraperitoneal mice macrophages were obtained as previously described [41] and cultured in DMEM high-glucose, +L-glu, supplemented with 10% FBS (inactivated). The procedure was performed minimizing the distress and pain for animals following the NIH guidance and animal protocol approved by UTEP's Institutional Animal Care and Use Committee (IACUC).

Evaluation of the toxicity on mammalian cell lines

Alamar Blue assay—The toxicity to human osteoblasts, fibroblasts, and murine macrophages was determined using Alamar Blue, as previously described [42]. I.P. macrophages were tested at drug concentrations of 0.0586, 0.117, 0.234, 0.468, 0.937, 1.87, and 3.75 μM; RAW 264.7 macrophages at 0.117, 0.234, 0.468, 0.937, 1.87, 3.75, and 7.5

M. H207 (human fibroblasts) and U20S (human osteoblasts) were assayed at 0.117, 0.234, 0.468, 0.937, 1.87, 3.75, 7.5, 15, 30, 60, and 120 M of the drugs.

Luciferase assay - Leishmania major and Trypanosoma cruzi—The anti-parasitic activity of complexes **1**-**6** was determined using the *L. major* strain Friedlin clone V1 (*Lm*-luc) and *T. cruzi* Y strain (*TcLuc-RAM*). The drugs (stock solutions in DMSO) were tested in a concentration range from 0.0586 to 30 M; 1 per well was added (1% DMSO final concentration) to 96-well microplates using an Eppendorf epMotion 5070 automated pipetting system. *L. major* promastigotes and *T. cruzi* epimastigotes (10^6/well) were added, and parasite survival was assessed by luciferase activity with the substrate 5 fluoroluciferin (ONE-Glo Luciferase Assay System, Promega) after 96 h incubation at 28°C, using a luminometer (Luminoskan, Thermo). The bioluminescent intensity was a direct measure of the survival of parasites. The assay was performed in triplicate in three independent experiments, from which the lethal doses (LD_{50}) were determined for each drug.

In vitro evaluation of compounds 3-5 by high-content imaging assay: infectivity experiments—To mimic in vivo infections, intraperitoneal mice macrophages were placed in a microplate and infected with the metacyclic promastigote form of *L. major* strain Friedlin clone V1, followed by treatment with complexes **3-5**. The macrophages were seeded at a density of 1×10^6 in a 96-well flat-bottom microplate for 8 h prior to infection. The metacyclic promastigotes of *L.* major were collected and washed twice with PBS at pH 7.2 (1,600 *g* for 10 min) and their concentration was adjusted to 8×10^6 parasites/ml. The infection of macrophage cells was performed for 24 h, at a ratio of 8 parasites per macrophage, in triplicate. After 24 h, the cells were washed twice with PBS, and the infected cells were incubated with the drug. Several concentrations (0.058 M to 3.75 M) and incubation times were assayed. The cells were fixed with 4% paraformaldehyde and stained with Alexa Fluor 488 Phalloidin and DAPI. The number of infected cells and amastigotes was determined by HCIA using a BD Pathway Bioimager microplate confocal microscope [30, 43]. Subsequently, the infection index was calculated from the mean of triplicate values by multiplying the percentage of infected cells by the constraint used in the HCIA assay, which was of 5 parasites per macrophage (adaptation from Lonardoni et al. 2000). The infection index is thus directly proportional to the % of infected cells. The statistical significance was determined.

Results and Discussion

Synthesis and characterization of complexes 1-6

The complex *cis*-[$Ru^{II}Cl_2(DMSO)_4$] reacts smoothly with 1 eq of KTZ in CH_2Cl_2 at room temperature to afford *cis-fac*-[$Ru^{II}Cl_2(DMSO)_3$(KTZ)] (**1**). The 2,2 bipyridine (bipy) derivative *cis*-[$Ru^{II}Cl_2$(bipy)(DMSO)(KTZ)] (**2**), on the other hand, is best prepared by reaction of *cis*-[$Ru^{II}Cl_2(DMSO)_4$] with bipy under reflux in THF to produce the intermediate *cis-cis*-[$Ru^{II}Cl_2(DMSO)_2$(bipy)], followed by addition of an equimolar amount of KTZ and refluxing overnight in chloroform (Scheme 1). After appropriate work-up, the complexes are isolated in high yields as air stable, light-yellow and light-brown solids, respectively. NMR data (^1H, ^{13}C, COSY, NOESY and HSQC) are consistent with coordination of KTZ through the N1 atom of the imidazole moiety (for assignments of all ^1H and ^{13}C NMR signals, see Material and Methods Section; atom numbering in Fig. 1). For instance, the signals corresponding to H_2 and H_5 of coordinated KTZ in complex **1** are significantly shifted to higher frequencies (= 1.00 and 0.75 ppm) with respect to uncomplexed KTZ. The 2D NOESY spectrum reveals short distances between H_2 and H_5 and two of the three coordinated DMSO molecules in accord with the *cis,fac* stereochemistry expected by analogy with known related compounds [44].

The ligand arrangement is further confirmed by the NOE interactions observed between all methyl groups of the DMSO molecules (Fig. 2), in good agreement with what we observed for the analogous CTZ compound *cis,fac*-[$Ru^{II}Cl_2(DMSO)_3(CTZ)$] [30]. Alessio *et al.* have established that the formation of the alternative *cis,mer* isomer is not to be expected e.g. for analogous ruthenium benzimidazole complexes, from the known reactivity of *cis*-[$Ru^{II}Cl_2(DMSO)_4$] [45]. Compound **2** also shows chemical shifts for the imidazole protons that agree with N-coordination to ruthenium. Interligand Overhauser effect (ILOE) analysis of **2** (Fig. 2) indicates a configuration where the bipy ligand adopts a *trans* disposition with respect to both chloride atoms, and a *cis* configuration to the KTZ and DMSO ligands. This is further confirmed by the observed NOE interactions of the *ortho* protons of bipy with both imidazole protons (H_2 and H_5) and with the methyl groups of DMSO.

The organometallic □-arene-Ru-KTZ derivatives, in turn, were synthesized from appropriate well-known starting materials, as summarized in Scheme 2. Addition of two eq of KTZ to a suspension of [Ru^{II}(□-*p*-cymene)$Cl_2]_2$ in acetone at room temperature readily produces [Ru^{II}(□-*p*-cymene)Cl_2(KTZ)] (**3**) as a light brown precipitate. Similarly, chloride abstraction from [Ru^{II}(□-*p*-cymene)Cl(en)][BF_4] or [Ru^{II}(□-*p*-cymene)Cl(acac)] using $AgBF_4$, followed by addition of KTZ yielded the corresponding cationic derivatives [Ru^{II}(□-*p*-cymene)(en)(KTZ)][$BF_4]_2$ (**4**), and [Ru^{II}(□-*p*-cymene)(acac)(KTZ)][BF_4] (**6**). The complex [Ru^{II}(□-*p*-cymene)(bipy)(KTZ)][$BF_4]_2$ (**5**) was prepared from [Ru^{II}(□-*p*-cymene)$Cl_2]_2$ by treatment with 4 eq of $AgBF_4$ followed by addition of bipy and KTZ. All the new compounds have been well characterized by 1D/2D ^1H and ^{13}C NMR spectroscopy and microanalysis; the complete assignment of all ^1H and ^{13}C NMR signals for the four complexes is presented in the Materials and Methods Section. Additionally, the crystal and molecular structure of compound **3** was determined by X-ray diffraction (*vide infra*).

X-ray structure of [$Ru^{II}(\eta^6$-p-cymene)Cl_2(KTZ)] (3)

Crystals of complex **3** were obtained by slow evaporation of a CH_2Cl_2 solution. Table 1 lists the crystal and refinement data; the molecular structure is shown in Fig. 3 and the most relevant bond lengths and angles are contained in Table 2. The coordination around the ruthenium center is essentially a “piano-stool” distorted octahedral arrangement that includes the *p*-cymene ring, two chlorides and the N1 atom of the imidazole moiety of KTZ. The average Ru-C and Ru-Cl distances of 2.17 Å and 2.42 Å, respectively, as well as the Ru-N bond length of 2.115(4) and corresponding angles are within the normal range for similar molecules [46], and specifically for $Ru^{II}Cl_2(BTZ)_2$ (BTZ is the bromo analogue of CTZ) [18], and for the analogous CTZ compound [Ru^{II}(□-*p*-cymene)Cl_2(CTZ)] recently reported by us [30]. Other structural features of the KTZ ligand are unremarkably analogous to those of the free molecule [47].

Biological Activity

The activity of the new Ru-KTZ complexes **1**-**6** on the proliferation of in vitro cultures of promastigotes of *L. major* and epimastigotes of *T. cruzi*, was tested at various concentrations, in comparison with uncomplexed KTZ and with Ru compounds of similar structures but not containing KTZ, namely Na[*trans*-$Ru^{III}Cl_4(DMSO)_2$] (**C1**), *cis*-[$Ru^{II}Cl_2(DMSO)_4$] (**C2**) and [□-Ru^{II}(*p*-cymene)$Cl_2]_2$ (**C3**). Cytotoxicity assays were also performed on human fibroblasts and osteoblasts, as well as murine macrophages and intraperitoneal macrophages, in order to ascertain the selectivity of the compounds for attacking the parasites of interest over normal mammalian cells. The results of all bioassays are collected in Table 3 and Fig. 4. Uncomplexed KTZ displays a good in vitro activity and selectivity against promastigotes of *L. major* (LD_{50} 1.9 □M; S.I. above 63). The Ru complexes not containing KTZ (**C1**-**C3**) are in turn much less active than KTZ toward leishmania (LD_{50} 12-15 □M). However, by combining KTZ and Ru in single molecules, as

in compounds **3**, **4**, and **5**, the desired metal-drug synergy is achieved. The activity of the Ru-KTZ complexes (LD_{50} 0.8-1.5 μM) is about twice that of KTZ alone and at least ten times that of the structurally analogous Ru complex **C3** not containing KTZ (LD_{50} 12.5 μM). Importantly, the enhancement of the anti-leishmanial activity of KTZ by Ru is accompanied by a significant increase in selectivity with respect to human cells (S.I. 78-150).

In order to further assess the medicinal potential of the new Ru-KTZ complexes **3-5**, additional tests were performed against the therapeutically more relevant infectious intracellular amastigote form of *L. major,* by means of a high-content imaging assay (HCIA) on infected intraperitoneal mice macrophages (see Materials and Methods Section).

As shown in Fig. 5a, complexes **3**-**5** showed significant inhibition of the proliferation of intracellular amastigotes, as compared to the negative control (culture medium with 1% DMSO), within the range of concentrations employed (0.11-3.75 μM). For complex **3,** inhibition reached about 50% at a concentration of 0.1 μM. In contrast, a concentration of 5 μM of the standard drug amphotericin B was needed to reach 30% inhibition. Also importantly, no significant cytotoxicity for intraperitoneal mouse macrophages was observed for compounds **3**-**5** within the same concentration range (Fig.5b).

Concerning *T. cruzi* epimastigotes, KTZ alone displays a significant activity and selectivity, similar to those observed in the case of *L. major* (Table 3). The Ru complexes **C1**-**C3** not featuring a KTZ ligand and complex **6**, containing the acac ligand, are essentially non-toxic to the parasites. Complex **3** displays the best performance of this series, with an activity and selectivity (LD_{50} 1.39 μM; S.I. > 86) comparable to those observed for KTZ (LD_{50} 1.5 μM; S.I. > 82); the efficacy decreases for complexes **4** and **5**.

It is interesting to note that [Ru^{II}(η⁶-*p*-cymene)Cl_2(KTZ)] (**3**), the most active complex reported herein against both types of parasites, is structurally analogous to [Ru^{II}(η⁶-*p*-cymene)Cl_2(CTZ)], the most effective member of the arene-Ru-CTZ family reported by us before [30]. In an early paper concerning the related compound $RuCl_2(CTZ)_2$ we proposed a dual-target anti-*T. cruzi* mechanism, which involves initial aquation of the chloride ligands to form cationic active species $[RuCl(H_2O)(CTZ)_2]^+$ and/or $[Ru(H_2O)_2(CTZ)_2]^{2+}$. The hydrolysis is likely followed by interactions of the aqua species with biomolecules in the cellular medium that lead to dissociation of CTZ. Once liberated from the metal, CTZ exerts its known SBI action. The remaining Ru-containing moiety binds covalently to the DNA of the parasite as a second target and the dual action leads to high activity and low toxicity [18]. We believe that an analogous mechanism involving initial activation by aquation is operative for [Ru^{II}(η⁶-*p*-cymene)Cl_2(CTZ)] [30] and for the present case of [Ru^{II}(η⁶-*p*-cymene)Cl_2(KTZ)]. In agreement with this hypothesis, electrical conductance measurements for [Ru^{II}(η⁶-*p*-cymene)Cl_2(KTZ)] (**3**) (10^{-3} M in 10% aqueous DMSO) reveal a value typical of two ions in solution (Λ = 115 μS.cm^{-1} immediately after dissolution, increasing slowly to 130 μS.cm^{-1} within 72 h.). This is consistent with one chloride ligand exchanging rapidly with water to form [Ru^{II}(η⁶-*p*-cymene)Cl(KTZ)(H_2O)][Cl] (**3a**), presumably the active species. The UV-visible spectrum of solutions of complex **3** (Supplementary Information) also remains unchanged over a period of 72 h, consistent with the rapid formation of the cationic aqua species **3a**. Additionally, diagnostic NMR signals around 7.8 ppm, assigned to H_2 of coordinated KTZ in complex **3**, are present in the spectrum over a period of 72 h while the spectral features typical of free KTZ are not observed; no broadening of the spectra due to the presence of paramagnetic Ru^{III} species could be detected over the same period of time. The combined conductivity and spectral data show that in aqueous DMSO medium at neutral pH: (i) the chlorides are labile; (ii) KTZ does not dissociate to any appreciable extent; and (iii) no oxidation to paramagnetic Ru^{III} takes place.

Hydrolysis of one chloride ligand to form the cationic aqua species **3a** appears to be a prerequisite for biological activity, and dissociation of KTZ probably takes place but only upon further interactions of **3a** with biomolecules within the parasite cell. [Ru^{II}(η^6-*p*-cymene)(en)(KTZ)][BF_4]$_2$ (**4**) and [Ru^{II}(η^6-*p*-cymene)(bipy)(KTZ)][BF_4]$_2$ (**5**) are less active than **3** against *L. major* and *T. cruzi*; the lower performance observed may be a consequence of the presence of chelating ethylenediamine or bipyridine ligands, not susceptible to easy exchange with water. The antiparasitic activity observed could be related to a combination of the SBI action of dissociated KTZ and the ability of N-chelating ligands on the remaining Ru-containing fragment to promote interactions with DNA through hydrogen bonding in the case of ethylenediamine [48, 49], or by π-stacking interactions for bipyridine [50, 51]. Complex **6**, on the other hand, does not contain any ligands that can be easily hydrolyzed or that promote DNA interactions, and in consequence, it is the least effective of the organometallic species against *L. major* and essentially non-toxic to *T. cruzi*. The octahedral coordination complexes **1** and **2** are less active against *L. major* or *T. cruzi* than the organometallic derivatives **3**-**6**, also in agreement with the trend previously reported by us for analogous CTZ derivatives [30]. Further mechanistic studies on the chemical and biological pathways that lead to the antiparasitic action of these Ru-based drugs are currently in progress in our laboratories and will be reported separately.

Conclusion

In an effort to discover new metal-based agents against leishmaniasis and Chagas disease, six new ruthenium-ketoconazole complexes were synthesized and characterized, namely *cis*-*fac*-[$Ru^{II}Cl_2(DMSO)_3$(KTZ)] (**1**) and *cis*-[$Ru^{II}Cl_2$(bipy)(DMSO)(KTZ)] (**2**), [Ru^{II}(η^6-*p*-cymene)Cl_2(KTZ)] (**3**), [Ru^{II}(η^6-*p*-cymene)(en)(KTZ)][BF_4]$_2$ (**4**), [Ru^{II} (η^6-*p*-cymene)(bipy)(KTZ)][BF_4]$_2$ (**5**), and [Ru^{II}(η^6-*p*-cymene)(acac)(KTZ)][BF_4] (**6)**; the crystal structure of (**3**) was determined by x ray diffraction methods. In agreement with the metal-drug synergy that we have previously proposed, binding of KTZ to Ru^{II} in compounds **3**-**5** led to a marked increase of the activity toward promastigotes and intracellular amastigotes of *L. major*, when compared with uncomplexed KTZ, or with similar Ru compounds not containing KTZ. Importantly, the selectivity of compounds **3**-**5** toward leishmania parasites, in relation normal human cells, is also higher than those observed for the individual constituents of the drug. When tested against *Trypanosoma cruzi* epimastigotes, some of the organometallic complexes displayed an activity and selectivity comparable to those of free KTZ. A dual-target mechanism is suggested to account for the antiparasitic properties of these complexes by analogy with a previous proposal for the related complex $RuCl_2(KTZ)_2$. Conductivity and spectroscopic data for complex **3** show that in aqueous media at neutral pH: (i) the chlorides are labile; (ii) KTZ does not dissociate to any appreciable extent; and (iii) no oxidation to paramagnetic Ru^{III} takes place. Hydrolysis of the chloride ligands to form cationic aqua species appears to be a prerequisite for biological activity and dissociation of ketoconazole probably takes place but only upon further interactions of the active species with biomolecules within the parasite cell.

Supplementary Material

Refer to Web version on PubMed Central for supplementary material.

Acknowledgments

We thank the staff of the Cell Culture and High Throughput Screening (HTS, #20) Core Facility of UTEP for services and facilities provided; this core facility is supported by NIMHD Grant #G12MD007592. We thank the BBRC for the small grant (NIMHD/G12MD007592) and the University of Texas URI for a grant (to R.A.M.). M.A.V. was supported by NIH-RISE (2R25GM069621-10). We also thank the NIH for support through Grant

#5SC1GM089558 (to R.A. S-D.) and the National Science Foundation (CHE-0619638) for the acquisition of an X-ray diffractometer for Columbia University.

Abbreviations Used

acac	acetylacetonate
bipy	bipyridine
CTZ	clotrimazole
en	ethylenediamine
dppz	(dipyrido[3,2-a:2 B Ec]phenazine)
DMEM	Dulbecco's modified Eagle's medium
FBS	fetal bovine serum
HCIA	high content imaging assay
ILOE	interligand Overhauser effect
KTZ	ketoconazole
PCR	polymerase chain reaction
SBI	sterol biosynthesis inhibitor

References

1. WHO. Control of leishmaniases. Geneva: 2010.
2. den Boer M, Argaw D, Jannin J, Alvar J. Clin Microbiol Infec. 2011; 17:1471–1477. DOI 10.1111/j.1469-0691.2011.03635.x. [PubMed: 21933305]
3. Barrett MP, Burchmore RJS, Stich A, Lazzari JO, Frasch AC, Cazzulo JJ, Krishna S. Lancet. 2003; 362:1469–1480. [PubMed: 14602444]
4. WHO. Control of Chagas disease. Geneva: 2002.
5. Dias JC, Silveira AC, Schofield CJ. Mem Inst Oswaldo Cruz. 2002; 97:603–612. [PubMed: 12219120]
6. Hotez PJ, Bottazzi ME, Franco-Paredes C, Ault SK, Periago MR. PLoS Negl Trop Dis. 2008; 2:e300. DOI 10.1371/journal.pntd.0000300. [PubMed: 18820747]
7. Kirchhoff LV. Adv Parasitol. 2011; 75:1–18. DOI 10.1016/B978-0-12-385863-4.00001-0. [PubMed: 21820549]
8. Sánchez-Delgado RA, Anzellotti A. Mini Rev Med Chem. 2004; 4:23–30. DOI 10.2174/1389557043487493. [PubMed: 14754440]
9. Sánchez-Delgado, RA.; Anzellotti, A.; Suárez, L. Met Ions Biol Syst. Siegel, H.; Siegel, A., editors. Marcel Dekker, Inc.; New York: 2004. p. 379-419.
10. Croft SL, Barrett MP, Urbina JA. Trends Parasitol. 2005; 21:508–512. DOI S1471-4922(05)00253-9 [pii] 10.1016/j.pt.2005.08.026. [PubMed: 16150644]
11. Urbina JA. Mem Inst Oswaldo Cruz. 2009; 104:311–318. DOI 10.1590/s0074-02762009000900041. [PubMed: 19753490]
12. Urbina JA. Drugs Fut. 2010; 5:409–419.
13. Urbina JA. Acta Tropica. 2010; 115:55–68. DOI 10.1016/j.actatropica.2009.10.023. [PubMed: 19900395]
14. Urbina JA, Docampo R. Trends Parasitol. 2003; 19:495–501. [PubMed: 14580960]
15. de Souza W, Fernandes Rodrigues JC. Interdisc Perspect Infec Dis. 2009:642502.
16. Roberts CW, McLeod R, Rice DW, Ginger M, Chance ML, Goad LJ. Mol Biochem Parasitol. 2003; 126:129–142. DOI S0166685102002803 [pii]. [PubMed: 12615312]

17. Sánchez-Delgado RA, Lazardi K, Rincon L, Urbina JA, Hubert AJ, Noels AN. J Med Chem. 1993; 36:2041–2043. DOI 10.1021/jm00066a014. [PubMed: 8336342]
18. Sánchez-Delgado RA, Navarro M, Lazardi K, Atencio R, Capparelli M, Vargas F, Urbina JA, Bouillez A, Noels AF, Masi D. Inorg Chim Acta. 1998; 275-276:528–540. DOI 10.1016/s0020-1693(98)00114-5.
19. Navarro M, Cisneros-Fajardo EJ, Lehmann T, Sánchez-Delgado RA, Atencio R, Silva P, Lira R, Urbina JA. Inorg Chem. 2001; 40:6879–6884. DOI 10.1021/ic0103087. [PubMed: 11754267]
20. Navarro M, Lehmann T, Cisneros-Fajardo EJ, Fuentes A, Sánchez-Delgado RA, Silva P, Urbina JA. Polyhedron. 2000; 19:2319–2325. DOI 10.1016/s0277-5387(00)00495-2.
21. Otero L, Vieites M, Boiani L, Denicola A, Rigol C, Opazo L, Olea-Azar C, Maya JD, Morello A, Krauth-Siegel RL, Piro OE, Castellano E, González M, Gambino D, Cerecetto H. J Med Chem. 2006; 49:3322–3331. DOI 10.1021/jm0512241. [PubMed: 16722651]
22. Vieites M, Otero L, Santos D, Olea-Azar C, Norambuena E, Aguirre G, Cerecetto H, González M, Kemmerling U, Morello A, Diego Maya J, Gambino D. J Inorg Biochem. 2009; 103:411–418. DOI 10.1016/j.jinorgbio.2008.12.004. [PubMed: 19187969]
23. Vieites M, Otero L, Santos D, Toloza J, Figueroa R, Norambuena E, Olea-Azar C, Aguirre G, Cerecetto H, González M, Morello A, Maya JD, Garat B, Gambino D. J Inorg Biochem. 2008; 102:1033–1043. DOI 10.1016/j.jinorgbio.2007.12.005. [PubMed: 18226837]
24. Demoro B, Sarniguet C, Sánchez-Delgado R, Rossi M, Liebowitz D, Caruso F, Olea-Azar C, Moreno V, Medeiros A, Comini MA, Otero L, Gambino D. Dalton Trans. 2012; 41:1534–1543. DOI 10.1039/C1DT11519G. [PubMed: 22138896]
25. Merlino A, Otero L, Gambino D, Coitiño EL. Eur J Med Chem. 2011; 46:2639–2651. DOI 10.1016/j.ejmech.2011.03.046. [PubMed: 21550147]
26. Navarro M, Gabbiani C, Messori L, Gambino D. Drug Discov Today. 2010; 15:1070–1078. DOI 10.1016/j.drudis.2010.10.005. [PubMed: 20974285]
27. Navarro M, Hernandez C, Colmenares I, Hernandez P, Fernandez M, Sierraalta A, Marchan E. J Inorg Biochem. 2007; 101:111–116. DOI 10.1016/j.jinorgbio.2006.08.015. [PubMed: 17055060]
28. Navarro M, Cisneros-Fajardo EJ, Marchan E. Arzneim Forsch. 2006; 56:600–604. [PubMed: 17009842]
29. Fricker SP, Mosi RM, Cameron BR, Baird I, Zhu Y, Anastassov V, Cox J, Doyle PS, Hansell E, Lau G, Langille J, Olsen M, Qin L, Skerlj R, Wong RSY, Santucci Z, McKerrow JH. J Inorg Biochem. 2008; 102:1839–1845. DOI 10.1016/j.jinorgbio.2008.05.010. [PubMed: 18684510]
30. Martínez A, Carreon T, Iniguez E, Anzellotti A, Sánchez A, Tyan M, Sattler A, Herrera L, Maldonado RA, Sánchez-Delgado RA. J Med Chem. 2012; 55:3867–3877. DOI 10.1021/jm300070h. [PubMed: 22448965]
31. Bennett MA, Huang TN, Matheson TW, Smith AK. Inorg. Synth. 1982; 21:74–78.
32. Crabtree RH, Pearman A J. J Organomet Chem. 1977; 141:325–330. DOI 10.1016/s0022-328x(00)90856-8.
33. Carmona D, Ferrer J, Oro LA, Apreda MC, Foces-Foces C, Cano FH, Elguero J, Jimeno ML. J Chem Soc Dalton Trans. 1990:1463–1476.
34. Evans IP, Spencer A, Wilkinson G. J Chem Soc Dalton Trans. 1973:204–209.
35. Toyama M, Inoue K-I, Iwamatsu S, Nagao N. Bull. Chem. Soc. Japan. 2006; 79:1525–1534.
36. Sheldrick GM (1981). University of Göttingen, Göttingen, Federal Republic of Germany
37. Sheldrick GM. Acta Crystallogr A. 2008; 64:112–122. DOI 10.1107/S0108767307043930. [PubMed: 18156677]
38. Camargo EP. Rev Inst Med Trop Sao Paulo. 1964; 12:93–100. [PubMed: 14177814]
39. Thalhofer CJ, Graff JW, Love-Homan L, Hickerson SM, Craft N, Beverley SM, Wilson ME. J Vis Exp. 2010; 41:e1980. DOI 1980 [pii] 10.3791/1980.
40. Uphoff CC, Drexler HG. Methods Mol Biol. 2005; 290:13–23. DOI 1-59259-838-2:013 [pii]. [PubMed: 15361652]
41. Capul AA, Hickerson SM, Barron T, Turco SJ, Beverley SM. Infect Immun. 2007; 75:4629–4637. [PubMed: 17606605]

42. Lara D, Feng Y, Bader J, Savage PB, Maldonado RA. J Parasitol. 2010; 96:638–642. [PubMed: 19958044]
43. Nohara LL, Lema C, Bader JO, Aguilera RJ, Almeida IC. Parasitol Int. 2010; 59:565–570. [PubMed: 20688189]
44. Henn M, Alessio E, Mestroni G, Calligaris M, Attia WM. Inorg Chim Acta. 1991; 187:39–50. DOI 10.1016/s0020-1693(00)82975-8.
45. Alessio E, Calligaris M, Iwamoto M, Marzilli LG. Inorg Chem. 1996; 35:2538–2545. DOI 10.1021/ic9509793. [PubMed: 11666467]
46. Vock CA, Scolaro C, Phillips AD, Scopelliti R, Sava G, Dyson PJ. J Med Chem. 2006; 49:5552–5561. DOI 10.1021/jm060495o. [PubMed: 16942028]
47. Peeters OM, Blaton NM, Gerber JG, Gal J. Acta Crystalogr E Struct Rep Online. 2004; 60:O367.
48. Chen H, Parkinson JA, Morris RE, Sadler PJ. J Am Chem Soc. 2003; 125:173–186. DOI 10.1021/ja027719m. [PubMed: 12515520]
49. Habtemariam A, Melchart M, Fernández R, Parsons S, Oswald IDH, Parkin A, Fabbiani FPA, Davidson JE, Dawson A, Aird RE, Jodrell DI, Sadler PJ. J Med Chem. 2006; 49:6858–6868. DOI 10.1021/jm060596m. [PubMed: 17154516]
50. Song H, Kaiser JT, Barton JK. Nat. Chem. 2012; 4:615–620. DOI 10.1038/nchem.1375. [PubMed: 22824892]
51. Lincoln P, Nordén B. J Phys Chem B. 1998; 102:9583–9594. DOI 10.1021/jp9824914.

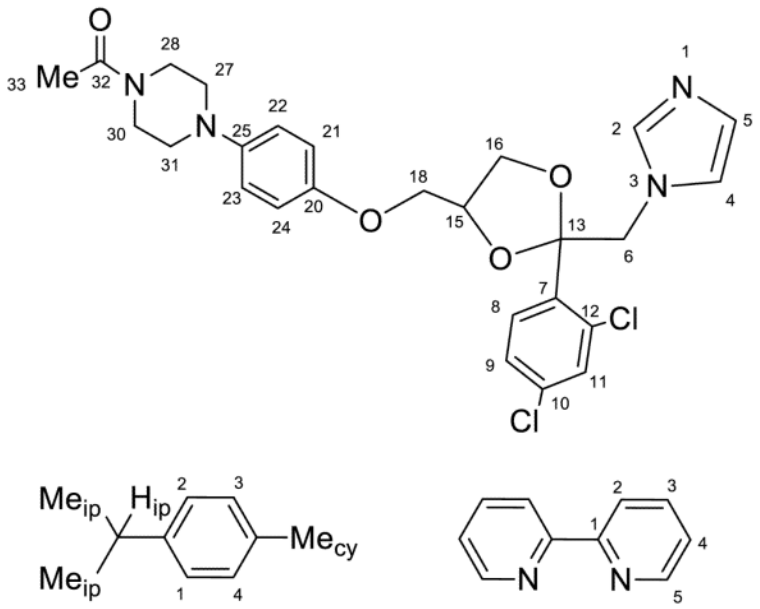

Figure 1.
Atom labeling used for ketoconazole, bipyridine and *p*-cymene.

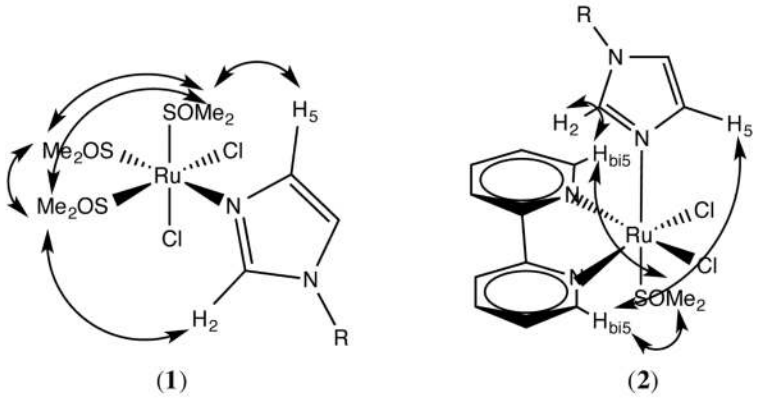

Figure 2.
Observed interligand Overhauser effects (ILOE) in compounds **1** and **2**

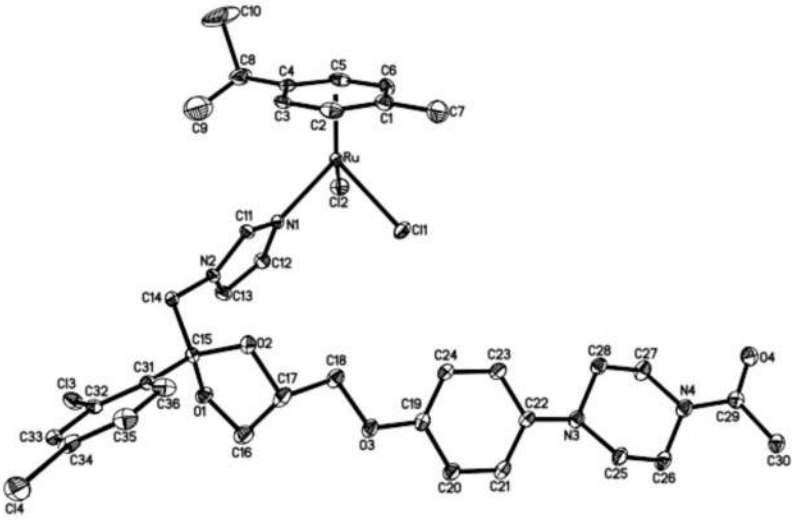

Figure 3.
Molecular structure of complex **3** (hydrogen atoms omitted for clarity)

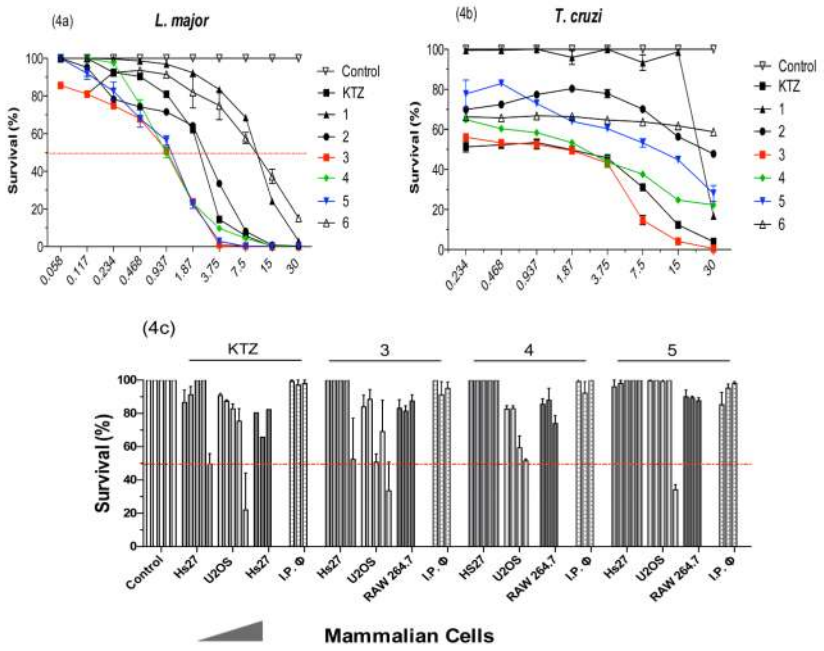

Figure 4.

Antiparasitic and cytotoxic activity of Ru-KTZ complexes. Control, culture medium with 1 % DMSO. (a) Promastigote forms of *L. major,* 96h. (b) Epimastigote forms of *T.* cruzi, 96h. (c) Selected data for cytotoxic activity in mammalian cells incubated with **3**, **4** and **5** at 0.117, 0.937, 3.75, and (for Hs27 and U2OS) 7.5, and 120 □M (details in Materials and Methods Section).

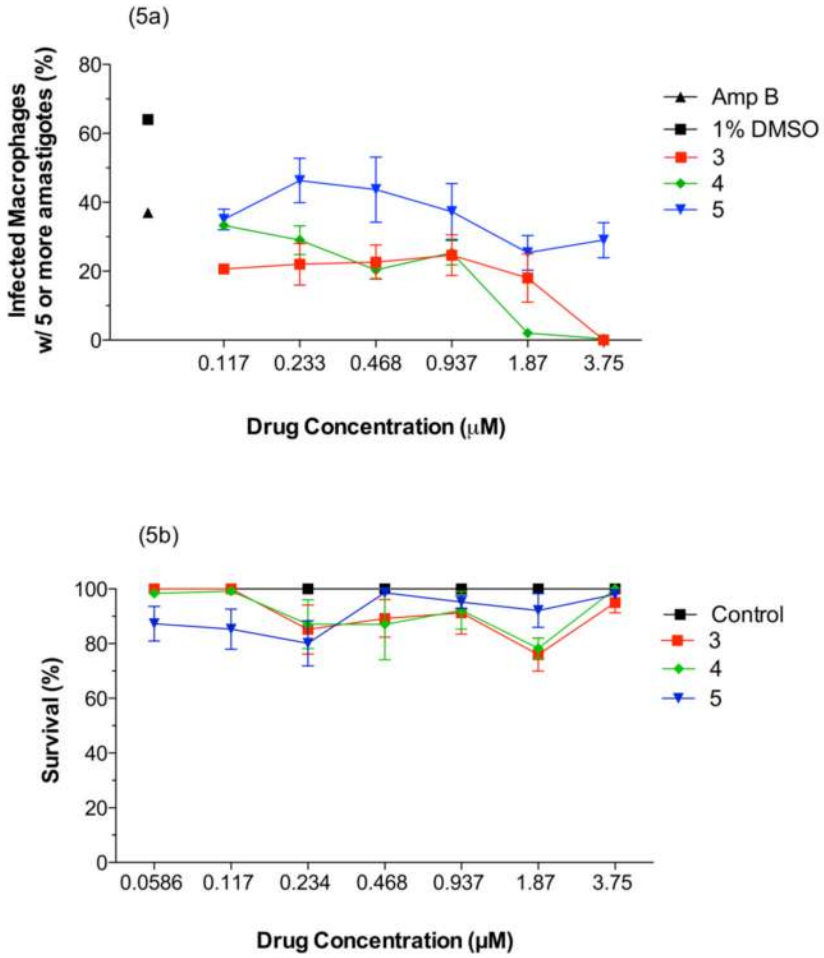

Figure 5.

(*a*) Activity of Ru-KTZ complexes **3**-**5** against intracellular amastigotes of *L. major* infecting intraperitoneal mouse macrophages. : negative control (culture medium with 1% DMSO). : positive control (treated with 5 M amphotericin B). (*b*) Cytotoxicity of complexes **3**-**5** toward intraperitoneal mouse macrophages.

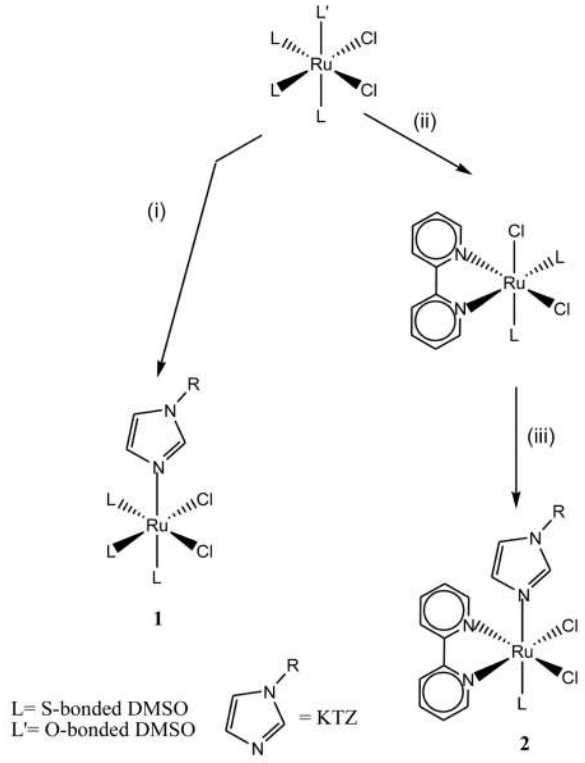

Scheme 1.
(i) KTZ, CH_2Cl_2, r.t. (ii) bipy, THF, reflux. (iii) KTZ, $CHCl_3$, reflux

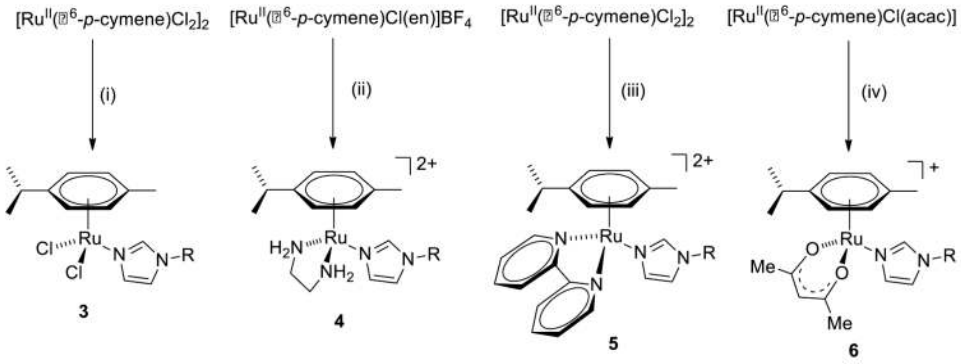

Scheme 2.

(i) KTZ, Me_2CO, r.t. (ii) (1) $AgBF_4$, Me_2CO, r.t. (2) KTZ. (iii) (1) $AgBF_4$, Me_2CO, r.t. (2) bipy, Me_2CO, r.t. (3) KTZ, CH_2Cl_2, r.t. (iv) (1) $AgBF_4$, Me_2CO, r.t. (2) KTZ, CH_2Cl_2, r.t.

Table 1

Crystal, intensity collection and refinement data

	[Ru^{II}(η6-*p*-cymene)Cl_2(KTZ)] (3)
Lattice	Monoclinic
Formula	C_{37} H_{44} Cl_6 N_4 O_4 Ru
Formula weight	922.53
Space group	$P2_1/c$
a / Å	13.3597(6)
b / Å	24.4419(12)
c / Å	12.9754(6)
α / °	90.00
β / °	109.3120(10)
γ / °	90.00
V / $Å^3$	3998.5(3)
Z	4
Temperature (K)	125(2)
Radiation (λ Å)	0.71073
ρ(cald.) Mg/m^3	1.532
Absn. Coeff. / mm^{-1}	0.837
F(000)	1888
Crystal size / mm	0.19 × 0.14 × 0.03
θrange, deg.	2.35 to 29.1°
Reflections collected	63473
Indep. reflections	12207 (R_{int} = 0.0951)
R_1 [*I* > 2 σ(*I*)]	0.0676
wR_2	0.1625
R_1 (all data)	0.1237
wR_2 (all data)	0.1820
GOF	1.010

Table 2

Selected bond lengths (Å) and angles (deg) for complex **3**

Ru–Cl 1	2.408(1)	$Ar_{centroid}$–Ru–Cl2	125.53
Ru–Cl2	2.422(1)	$Ar_{centroid}$–Ru–N1	129.55
Ru–N1	2.115(4)	Cl1–Ru–Cl2	87.52(4)
Ru–$Ar_{centroid}$	1.668	N1–Ru–Cl1	84.6(1)
$Ar_{centroid}$–Ru–Cl 1	128.52	N1–Ru–Cl2	86.7(1)

Table 3

In vitro antiparasitic activity of controls and Ru-KTZ complexes against promastigotes of *L. major* and epimastigotes of *T. cruzi*, and cytotoxic activity on mammalian cells (p-value <0.0001). Hs27: human fibroblast; U205: human osteoblasts; RAW 264.7: mice macrophages;IP : intraperitoneal macrophages

Compound	*L. major* (M)[1] [Rel. Act.][2] / (S.I.)[3]	*T. cruzi* (M)[1] [Rel. Act.][2] / (S.I.)[3]	Mammalian Cells M)[4]			
			Hs27	U2O5	RAW 264.7	IP
C1	15.36 ± 3.68 [0.12] (> 0.5)	> 30	>7.5		>7.5	>7.5
C2	13.23 ± 4.48 [0.14] (> 0.6)	> 30	>7.5		>7.5	>7.5
C3	12.52 ± 3.34 [0.15] (> 0.6)	> 30	>7.5		>7.5	>7.5
KTZ	1.9 ± 0.5 [1.0](> 63)	1.5 ± 2.9 [10] (> 82)	>120	120	>7.5	>3.5
1	9.30 ± 3.66 [0.2]	24.8 ± 2.9 [0.9]	ND		ND	ND
2	2.34 ± 1.25 [0.8]	28.36 [0.9]	ND		ND	ND
3	0.8 ± 1.32 [>2.4] (> 150)	1.39 ± 2.32 [1.04] (> 86)	>120	120	>7.5	>3.5
4	1.16 ± 0.52 [1.6](> 103)	2.28 ± 0.26 [0.64] (> 53)	>120	>120	>7.5	>3.5
5	1.53 ± 0.84 [1.2] (>78)	8.00 ± 2.96 [0.18](> 15)	>120	120	>15	>3.5
6	9.53 ± 6.3 [0.2]	> 30	ND		ND	ND

[1] LD_{50}: Median lethal dose calculated with 95% confidence interval; ± values are the estimated LD_{50} interval.

[2] [Rel. Act.]: Relative Activity (LD_{50} of KTZ)/(LD_{50} of Ru-KTZ complex)

[3] S.I.: Selectivity index (IC_{50} in Hs27 human cells)/(LD_{50} in parasites)

[4] IC_{50}: Median inhibitory concentration